Convective heat transfer from a rotating or nonrotating axisymmetric body

T.-Y. Wang
Department of Mechanical Engineering, Mingchi Institute of Technology, Taiwan, Republic of China

An analysis of steady laminar mixed-convection heat transfer from a rotating or nonrotating axisymmetric body is presented. A mixed-convection parameter is proposed to serve as a controlling parameter that determines the relative importance of the forced and the free convection. In addition, a rotation parameter is introduced to indicate the relative contributions of the flow forced convection and the rotational forced convection. The values of both these two parameters lie between 0 and 1. Furthermore, the coordinates and dependent variables are transformed to yield computationally efficient numerical solutions that are valid over the entire range of mixed convection from the forced-convection limit (rotating or nonrotating bodies) to the pure free-convection limit (nonrotating bodies) and the entire regime of forced convection from the pure flow forced-convection limit (nonrotating bodies) to pure rotational forced-convection limit (rotating bodies). The effects of mixed-convection intensity, body rotation, fluid suction or injection, and fluid Prandtl number on the velocity profiles, the temperature profiles, the skin-friction parameter, and heat transfer parameter are clearly illustrated for both cases of buoyancy assisting and opposing flow conditions.

Keywords: rotating or nonrotating bodies; mixed convection parameter; rotating parameter; fluid suction or injection

Introduction

The thermal flow-field analysis of spinning axisymmetric bodies in a mixed convection flow is important for numerous industrial applications. Examples include wire or fiber coating, transpiration cooling, projectile behavior, and rotary machine design. Body rotation enhances convection heat transfer because centrifugal forces push the fluid near the surface outward, which is then replaced by cooler or warmer fluid depending upon the wall temperature. Momentum and heat transfer rates may also be affected by the buoyancy force, which assists the forced flow for heated surfaces and retards in the case of cooled surfaces when the fluid is moving upwards against the gravitational force. If the wall of the submerged body is porous or perforated, fluid at a prescribed temperature can be injected into the boundary layer or fluid at the wall surface can be withdrawn. These additional mass transfer processes may measurably alter the local skin-friction coefficient and the local Nusselt number.

Simplified forms of the present system have been extensively analyzed in the past. For example, Chao and Greif (1974) assumed a quadratic velocity profile to study the forced-convection heat transfer along rotating bodies. Lee et al. (1978) applied a Merk series-expansion technique to analyze the momentum and heat transfer rates through laminar boundary layers over rotating isothermal bodies with revolution of arbitrary shape. Rajasekaran and Palekar (1985) also used Merk's series expansion to consider mixed-convection flow past a rotating sphere. Lien et al. (1986) extended the work done by Lee et al. to include the effect of wall mass transfer in the analysis of pure forced, pure free, and mixed thermal convection about a rotating sphere. Huang and Chen (1987) studied the influence of Prandtl number and surface mass transfer on a steady, laminar, free-convection flow over a sphere. Kleinstreuer and Wang (1989) investigated mixed thermal convection from porous bodies placed in non-Newtonian fluids. Very recently, a general analysis of steady mixed-convection heat transfer between a quiescent fluid and a rotating or nonrotating cone has been presented by Wang (1991). With the exception of Wang (1991), in all previous investigations the condition considered was pure forced convection, pure free convection, or mixed convection for only a limited range of Richardson numbers from a rotating axisymmetric body, and somewhat restrictive series expansions were employed to solve particular boundary-layer equations.

In the present analysis of convective heat transfer from a rotating or nonrotating axisymmetric body, a mixed-convection parameter and a rotation parameter are introduced. These two dimensionless groups serve, respectively, as a controlling parameter that determines the relative importance of the forced and the free convection and as an index that indicates the relative contributions of the flow forced convection and the rotational forced convection. The numerical solutions are valid over the entire regime of mixed convection intensity from pure free convection ($\zeta = 0$) to pure forced convection ($\zeta = 1$) and over the entire region of forced convection from the pure flow forced-convection limit (nonrotating bodies, RP = 0) to the pure rotational forced-convection limit (rotating bodies, RP = 1).

Address reprint requests to Professor Wang at the Department of Mechanical Engineering, Mingchi Institute of Technology, 84 Gungjuan Rd., Taishan, Taipei, Taiwan 24306, Republic of China.

Received 29 May, 1992; accepted 10 March 1993

Analysis

Modeling equations for an axisymmetric body

Consider steady laminar boundary-layer flow of a Newtonian fluid past a spinning permeable body at constant wall temperature. The axis of body rotation is parallel to the free-stream velocity. The fluid properties are considered to be constant except that the density variations within the fluid are allowed to contribute to the buoyancy force. When the wall temperature is higher than the ambient temperature, i.e., $T_w > T_\infty$ or $Z = 1$, the buoyancy force will aid the upwardly directed uniform stream, and when $T_w < T_\infty$, or $Z = -1$, the resulting buoyancy force will retard the forced flow. Nonrotating coordinates are chosen where x is the distance measured along a meridian curve from the forward stagnation point and y is measured normal to the surface of the body (Figure 1). Neglecting wake effects and viscous dissipation, the boundary-layer equations with the Boussinesq assumption are

$$\frac{\partial}{\partial x}(ru) + \frac{\partial}{\partial y}(rv) = 0 \tag{1}$$

$$u\frac{\partial u}{\partial x} + v\frac{\partial u}{\partial y} - \frac{w^2}{r}\frac{dr}{dx} = u_e\frac{du_e}{dx} + Zg\beta|T - T_\infty|\sin\phi + \nu\frac{\partial^2 u}{\partial y^2} \tag{2}$$

$$u\frac{\partial w}{\partial x} + v\frac{\partial w}{\partial y} + \frac{uw}{r} = \nu\frac{\partial^2 w}{\partial y^2} \tag{3}$$

$$u\frac{\partial T}{\partial x} + v\frac{\partial T}{\partial y} = \alpha\frac{\partial^2 T}{\partial y^2} \tag{4}$$

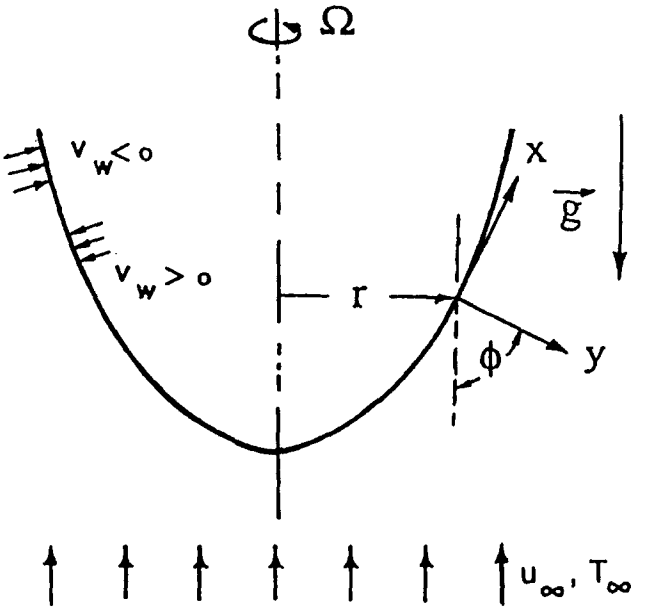

Figure 1 System schematics and coordinates

The associated boundary conditions are

at $y = 0$: $u = 0$, $v = v_w$, $w = r\Omega$, and $T = T_w$ = constant (5a)

as $y \to \infty$: $u = u_e(x)$, $w = 0$, and $T = T_\infty$ (5b)

where v_w is the wall velocity due to blowing or suction, r varied with x is the distance from the axis of symmetry to the surface of body, Ω is the angular velocity of the rotating body, and u_e is the outer velocity of fluid.

Notation

C_f	Local skin friction
F	Dimensionless stream function
G	Dimensionless velocity
g	Gravitational acceleration
h	Local heat transfer coefficient
k	Thermal conductivity
L	Characteristic length of axisymmetric body
MP	Mass transfer parameter
Nu	Nusselt number
Pr	Prandtl number
q	Local heat transfer rate
R	Radius of sphere
Ra	Raleigh number
RP	Rotation parameter
r	Distance from the axis of symmetry to the surface
T	Temperature
U	Pseudovelocity
u	Velocity component in the x-direction
v	Velocity component in the y-direction
w	Transverse velocity component
x	Streamwise coordinate
y	Coordinate normal to the surface
Z	Dimensionless parameter

Greek symbols

α	Thermal diffusivity
β	Thermal expansion coefficient
ζ	Mixed-convection parameter
η	Dimensionless coordinate
θ	Dimensionless temperature
λ	Dimensionless parameter
ν	Kinematic viscosity
ξ	Dimensionless coordinate
ρ	Density of fluid
τ	Shear stress
ϕ	Angle between the gravitational acceleration vector and the outward normal to the body surface
Ψ	Stream function
Ω	Angular velocity

Subscripts

e	Boundary-layer edge condition
w	Wall condition
∞	Ambient condition

The system of equations can be reduced using the stream function approach with

$$u = \frac{1}{r}\frac{\partial \Psi}{\partial y} \quad \text{and} \quad v = -\frac{1}{r}\frac{\partial \Psi}{\partial x} \tag{6a, b}$$

together with the transformations

$$\xi = \frac{x}{L}, \ \eta = \lambda \xi^{-1/2}(u_e/u_\infty)^{1/2} y/L \tag{7a, b}$$

$$\Psi = r\alpha\lambda\xi^{1/2}(u_e/u_\infty)^{1/2} F(\xi, \eta) - \int_0^x r v_w \, dx \tag{7c}$$

$$G = \frac{w}{r\Omega}, \quad \text{and} \quad \theta = \frac{T - T_\infty}{T_w - T_\infty} \tag{7d, e}$$

The dimensionless buoyancy parameter λ is defined as

$$\lambda = \mathrm{Re}^{1/2} + \mathrm{Ra}^{1/4} = \mathrm{Re}^{1/2}/(1 - \zeta) = \mathrm{Ra}^{1/4}/\zeta \tag{8}$$

where $\mathrm{Re} = (u_\infty L + L^2\Omega)/\nu$ and $\mathrm{Ra} = g\beta|T_w - T_\infty|L^3/(\alpha\nu)$ are the Reynolds number and the Raleigh number, respectively, with L being the characteristic length of the body. The mixed-convection parameter ζ, covering the entire domain of mixed convection from pure forced convection ($\zeta = 0$) to pure free convection ($\zeta = 1$), is defined as

$$\zeta = \mathrm{Ra}^{1/4}/(\mathrm{Re}^{1/2} + \mathrm{Ra}^{1/4}) \tag{9}$$

As a result, the continuity equation is automatically satisfied, and the momentum equations and energy equation are transformed to

$$\mathrm{Pr}F''' + B(\xi)FF'' - A(\xi)F'^2 + C(\xi, \zeta) + E(\xi)G^2 - \mathrm{MP}\, D(\xi)F'' + ZS(\xi, \zeta)\theta = \xi\left[F'\frac{\partial F'}{\partial \xi} - F''\frac{\partial F}{\partial \xi}\right] \tag{10}$$

$$\mathrm{Pr}G'' + B(\xi)FG' - H(\xi)GF' - \mathrm{MP}\, D(\xi)G' = \xi\left[F'\frac{\partial G}{\partial \xi} - G'\frac{\partial F}{\partial \xi}\right] \tag{11}$$

$$\theta'' + B(\xi)F\theta' - \mathrm{MP}\, D(\xi)\theta' = \xi\left[F'\frac{\partial \theta}{\partial \xi} - \theta'\frac{\partial F}{\partial \xi}\right] \tag{12}$$

The corresponding boundary conditions are

$$F(\xi, 0) = F'(\xi, 0) = 0; \ G(\xi, 0) = 1 \text{ and } \theta(\xi, 0) = 1 \tag{13a}$$

$$F'(\xi, \infty) = \mathrm{Pr}(1 - \zeta)^2(1 - \mathrm{RP}); \ G(\xi, \infty) = 0 \text{ and } \theta(\xi, \infty) = 0 \tag{13b}$$

The primes in the foregoing equations denote differentiation with respect to η. The system parameters include the rotation parameter

$$\mathrm{RP} = L^2\Omega/(u_\infty L + L^2\Omega) \tag{14}$$

which is valid over the entire regime of forced convection from the pure flow forced-convection limit (nonrotating bodies, RP = 0) to the pure rotational forced-convection limit (rotating bodies, RP = 1) and the mass transfer parameter

$$\mathrm{MP} = \frac{v_w L}{\alpha\lambda} \tag{15}$$

The new coefficients in Equations 10 to 12 are defined as

$$A(\xi) = (\xi/u_e)(du_e/d\xi) \tag{16a}$$

$$B(\xi) = (\xi/r)(dr/d\xi) + (1 + A(\xi))/2 \tag{16b}$$

$$C(\xi, \zeta) = \mathrm{Pr}^2(1 - \zeta)^4(1 - \mathrm{RP})^2 A(\xi) \tag{16c}$$

$$D(\xi) = \xi^{1/2}/(u_e/u_\infty)^{1/2} \tag{16d}$$

$$E(\xi) = \mathrm{Pr}^2\mathrm{RP}^2(1 - \zeta)^4(\xi/r)(dr/d\xi)((r/L)(u_e/u_\infty))^2 \tag{16e}$$

$$H(\xi) = 2(\xi/r)(dr/d\xi) \tag{16f}$$

$$S(\xi, \zeta) = \mathrm{Pr}\zeta^4\xi \sin \xi/(u_e/u_\infty)^2 \tag{16g}$$

The physical quantities of primary interest are the local skin-friction coefficient C_f and the local Nusselt number Nu. In order to deal with the whole region of mixed convection, the local skin-friction coefficient is defined as

$$C_f = \tau_w \Big/ \left(\frac{1}{2}\rho U^2\right) \tag{17}$$

where U is a pseudo- or reference velocity defined as

$$U = (u_\infty + L\Omega) + [g\beta|T_w - T_\infty|L]^{1/2} \tag{18}$$

Hence a dimensionless skin-friction parameter can be defined as

$$\mathrm{SFP} = \frac{1}{2}C_f\lambda = \frac{F''(\xi, 0)}{\mathrm{Pr}}\xi^{-1/2}(u_e/u_\infty)^{3/2}[(1 - \zeta)^2 + \zeta^2/\mathrm{Pr}^{1/2}]^{-2} \tag{19}$$

Similarly, with the definition of the local Nusselt number

$$\mathrm{Nu} = hL/k \tag{20}$$

a dimensionless heat transfer parameter can be defined as

$$\mathrm{HTP} = \frac{\mathrm{Nu}}{\lambda} = -\xi^{1/2}(u_e/u_\infty)^{1/2}\theta'(\xi, 0) \tag{21}$$

For a specific problem, the shape of the body $r(x)$, its characteristic length L, and the outer flow condition $u_e(x)/u_\infty$ have to be known—except for the pure free-convection case, because in that case the outer flow velocity is zero.

Application to a rotating sphere

For a sphere, $r(x) = R \sin(x/R)$ and $\phi = x/R = \xi$, where R is the radius of the sphere that corresponds to the characteristic length L. Two different edge velocity distributions may be used to carry out the calculations for the cases of pure forced convection and mixed convection. One is the potential flow

$$u_e/u_\infty = \tfrac{3}{2}\sin(x/R), \ x > 0 \tag{22}$$

and the other is based on measurements performed by Fage as given in White (1974):

$$u_e/u_\infty = 1.5\xi - 0.4371\xi^3 + 0.1481\xi^5 - 0.0423\xi^7, \ \xi > 0 \tag{23}$$

Equation 22 has been used for comparison purpose with previously published results. However, Equation 23 is assumed here for all other computations, since it describes the outer flow more realistically. The expression of Fage is valid for $x/R \ll 1.48$. Thus, the results presented here are terminated at $\phi = 90°$ or earlier when separation was imminent.

Numerical solution

The system of coupled nonlinear equations with the appropriate coefficients for the rotating permeable sphere were solved numerically with a modified version of Keller's box method described by Cebeci and Bradshaw (1977). The convergence criterion used was $|(\omega_{ij}^{k+1} - \omega_{ij}^k)/\omega_{ij}^{k+1}|_{\max} < 10^{-5}$, where ω^k and ω^{k+1} are the values of the kth and $(k+1)$th

iteration of F, F', F'', G, G'', θ, or θ'. The two-dimensional (2-D) grid is nonuniform in order to accommodate both the steep velocity and temperature gradients at the wall, particularly in the vicinity of the stagnation point, $\xi = 0$.

Numerical error testing has been accomplished by straightforward repeat calculations with finer meshes to check grid independence of the results and by local mesh refinement in the η-direction with smooth transition to the coarser region.

Results and discussion

Model verification

Since experimental data sets or analytical/numerical solutions are not available to check the accuracy of the present system, the results of special cases of the present study are compared with published data sets for the local skin-friction coefficient and the local Nusselt number of pure forced convection from a rotating sphere (cf. Tables 1 and 2). In addition, the values of $-\bar{\theta}'(\xi, 0)$ and $F''(\xi, 0)$ are compared with the results of Huang and Chen (1987) for pure free convection from a sphere (cf. Table 3). The results for these special case studies are very agreeable.

Velocity and temperature profiles around a sphere

The evolution of the profiles $F'(\xi, \eta) \approx u(x)/u_e$ from the pure forced-convection limit ($\zeta = 0$) to the pure free-convection limit ($\zeta = 1$) is presented in Figure 2 for a heated sphere. The transition of the profiles from one limit to the other is clearly shown in this figure.

To examine the effect of a cooled sphere ($Z = -1$) generating a buoyancy force that opposes the free stream, the dimensionless axial velocity

$$u/u_e = F'(\xi, \eta)/[\mathrm{Pr}\,(1 - \mathrm{RP})(1 - \zeta)^2] \tag{24}$$

is plotted in Figure 3. It is evident that the negative buoyancy force ($Z = -1$, $\zeta = 0.4$), which acts like an adverse pressure

Table 1 Comparison of $\frac{1}{2}C_f^* \mathrm{Re}^{1/2}$ for a rotating sphere with $\zeta = 0$ and MP = 0

ξ	RP* = 1.0			RP* = 4.0		
	Present method	Lien et al. (1987)	Lee et al. (1978)	Present method	Lien et al. (1987)	Lee et al. (1978)
0.474	1.2498	1.2499	1.2496	1.8174	1.8182	1.8170
0.951	1.8400	1.8400	1.8403	2.6357	2.6360	2.6362
1.215	1.7183	1.7185	1.7207	2.3979	2.3990	2.4032
1.374	1.4727	1.4732	1.4780	1.9770	1.9786	1.9882
1.486	1.2171	1.2173	1.2269	1.5362	1.5373	1.5644

$$\frac{1}{2} C_f^* \mathrm{Re}^{*1/2} = \frac{1}{2} C_{fi}/(1\text{-RP})^{3/2};\ \mathrm{RP}^* = \frac{4}{9}\left(\frac{\mathrm{RP}}{1\text{-RP}}\right)^2$$

Table 2 Comparison of $\mathrm{Nu}/\mathrm{Re}^{*1/2}$ for a rotating sphere with Pr = 1, $\zeta = 0$, and MP = 0

ξ	RP* = 1.0			RP* = 4.0		
	Present method	Lien et al. (1987)	Lee et al. (1978)	Present method	Lien et al. (1987)	Lee et al. (1978)
0	0.9583	0.9586	0.9588	1.0209	1.0213	1.0214
0.951	0.7991	0.7993	0.9778	0.8478	0.8480	0.8484
1.215	0.6962	0.6966	0.6961	0.7335	0.7339	0.7328
1.374	0.6191	0.6195	0.6171	0.6453	0.6459	0.6414
1.486	0.5554	0.5559	0.5510	0.5690	0.5698	0.5593

$$\mathrm{Re}^* = \frac{u_\infty R}{\nu};\ \mathrm{RP}^* = \frac{4}{9}\left(\frac{\mathrm{RP}}{1\text{-RP}}\right)^2$$

Table 3 Comparison of values of $-\bar{\theta}'(\xi, 0)$ and $f''(\xi, 0)$ for a sphere with $\zeta = 1$ and MP = 0

Pr	ϕ	$-\bar{\theta}'(\xi, 0)$		$f''(\xi, 0)$	
		Present method	Huang and Chen (1987)	Present method	Huang and Chen (1987)
0.7	0	0.4575	0.4574	0.7681	0.7678
	10	0.4564	0.4563	0.7658	0.7655
	30	0.4481	0.4480	0.7474	0.7471
	60	0.4194	0.4194	0.6865	0.6863
	90	0.3694	0.3694	0.5893	0.5892
7.0	0	0.9580	0.9581	0.5031	0.5034
	10	0.9559	0.9559	0.5017	0.5019
	30	0.9387	0.9389	0.4899	0.4901
	60	0.8803	0.8805	0.4512	0.4514
	90	0.7789	0.7792	0.3897	0.3898

$$-\bar{\theta}'(\xi, 0) = -\mathrm{Pr}^{1/4}\xi^{-1/2}(u_e/u_\infty)^{1/2}\theta'(\xi, 0)/\zeta$$
$$f''(\xi,0) = \mathrm{Pr}^{1/4}\xi^{-3/2}(u_e/u_\infty)^{-3/2}F''(\xi, 0)/\zeta$$

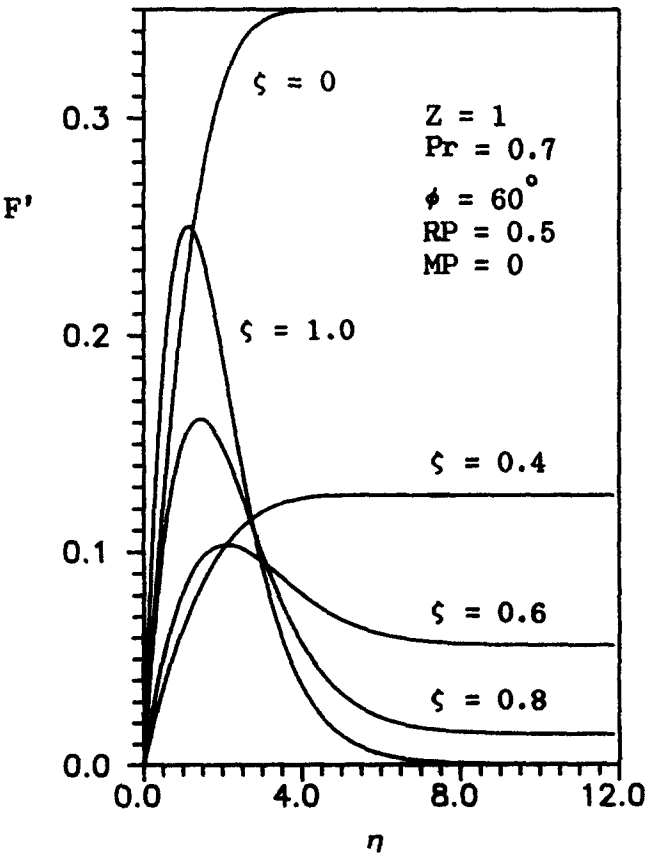

Figure 2 F' (η)-profiles for $\phi = 60°$ on a heated sphere for the entire free forced-convection range

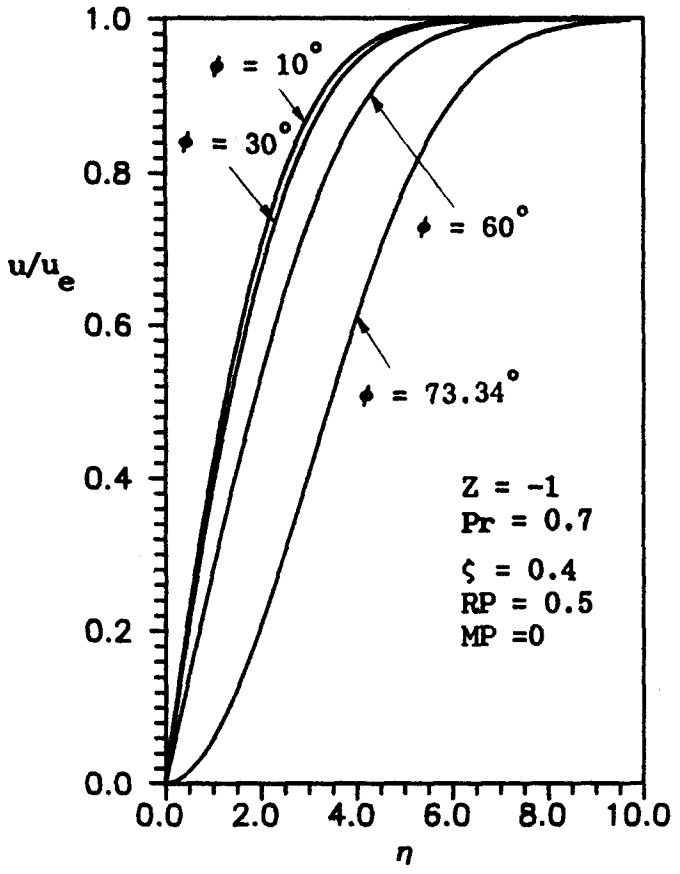

Figure 3 Streamwise velocity profiles at various locations for a cooled sphere

gradient, tends to retard the convection upward flow. It can be seen that for this particular set of system parameters, flow separation may occur for $\phi > 73.34°$ that is preceded by $(\partial u/\partial \eta) = 0$ at $\eta = 0$.

Representative temperature profiles on a rotating sphere at $\phi = 60°$ are shown in Figure 4. It is found that the dimensionless temperature gradients at the wall do not decrease monotonically with increasing buoyancy force. The reason is that θ' decreases in the forced-convection dominated regime since $\eta \approx (1 - \zeta)^{-1}$, and then θ' increases when the buoyancy force becomes dominant because $\eta \approx \zeta^{-1}$ in the free-convection dominated regime.

Effects of system parameters on local skin friction and Nusselt number distributions

The angular distributions of the skin-friction parameter (SFP) and the heat transfer parameter (HTP) for a rotating sphere are shown in Figures 5a and 5b, respectively. It is noted that in the figures $\phi = (x/R)(180/\pi)$, where R is the radius of the sphere. Proper selection of a pseudovelocity (cf., Equation 18) allows the simulation of SFP for the entire mixed-convection domain. Clearly, the buoyancy force helps to delay flow separation.

The effects of the rotation parameter RP on SFP and HTP are demonstrated in Figures 6a and 6b, respectively. As shown in these figures, an increase in rotating parameter generates a more uniform angular distribution of the skin-friction/heat transfer parameter because a stronger rotation motion causes a more active mixing process. In addition, stronger mixing also should increase heat transfer rates. The readers may have opposite opinions according to Figure 6b. However, although the pure flow forced-convection case (RP = 0) generates higher HTP at the stagnation point of the body ($\phi = 0$) than the pure rotational forced-convection case (RP = 1) does, the separation will occur imminently after $\phi = 90°$ for the pure flow forced-convection case (RP = 0), which can be seen from Figure 6a. Therefore, the overall heat transfer rate for the axisymmetric body for the pure rotational forced-convection case is higher than that of the pure flow forced-convection case.

Figures 7a and 7b depict the effects of fluid mass transfer at the heated sphere on SFP and HTP respectively, for different Prandtl numbers and a fixed mixed-convection parameter $\zeta = 0.6$. A general observation is that the impact of the mass transfer parameter is more pronounced at low Prandtl number. Furthermore, an increase in Prandtl number decreases the SFP and increases the HTP. It also can be seen from Figure 7b that suction increases the local Nusselt number, $\mathrm{Nu} \approx \theta'$, because the temperature gradient at the wall is greater when cooler fluid is drawn towards the heated surface. Conversely, injection of warm fluid decreases the Nusselt number.

The variations of skin-friction parameter and heat transfer parameter with the Prandtl number are illustrated in Figures 8a and 8b, respectively. As shown in Figure 8a, with a stronger influence of the fluid Prandtl number, the trends in SFP-values are reversed for $\phi \cong 60°$. For example, SFP increases with increasing Prandtl number on the front part of the sphere and then, in the rear part of the sphere, SFP decreases with increasing Prandtl number. The significant effect of Prandtl number on HTP can be seen from Figure 8b. An increase in Prandtl number increases the HTP values. The HTP profiles shift upward with higher Prandtl numbers because $\mathrm{Pr} \approx (1/\alpha)$

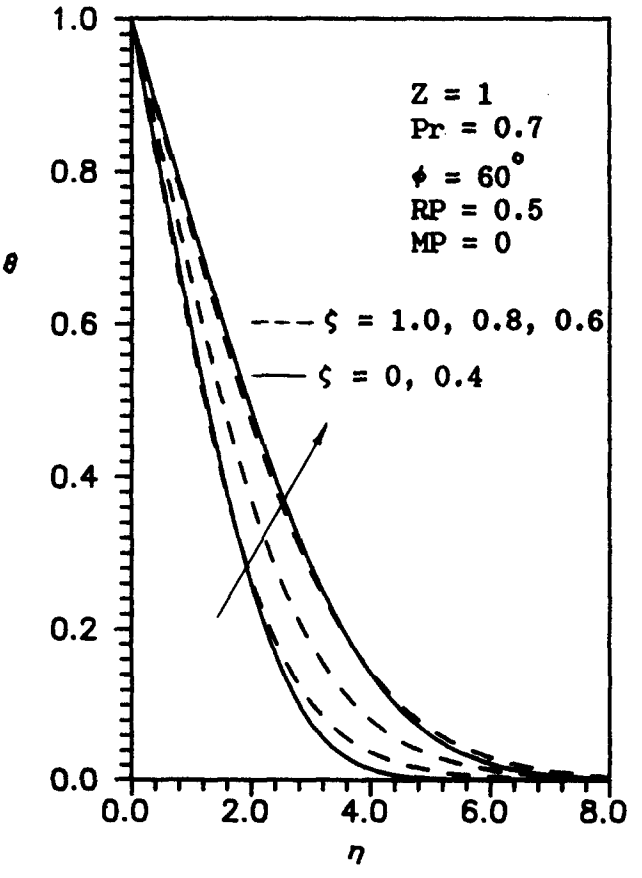

Figure 4 Representative temperature profiles at $\phi = 60°$ on a heated sphere for the entire free forced-convection range

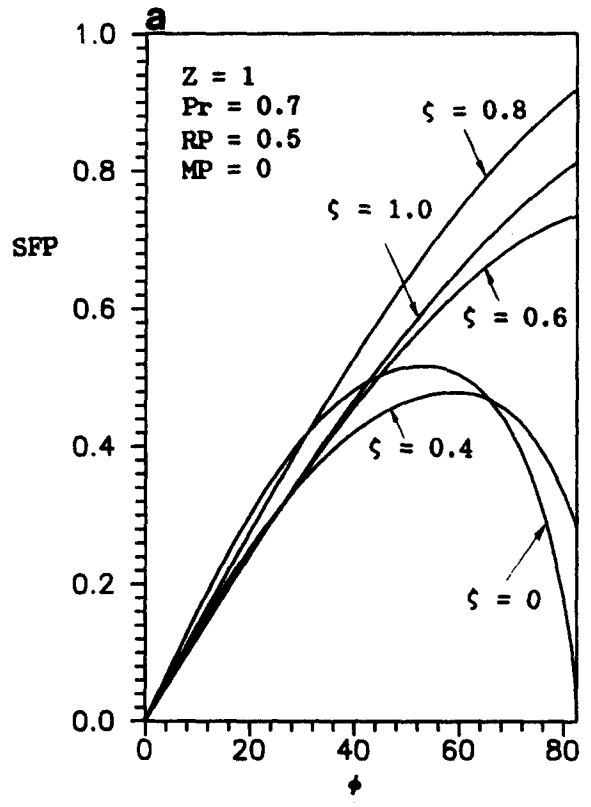

Figure 5a Angular distributions of the skin-friction parameter for a sphere covering the entire free forced-convection range

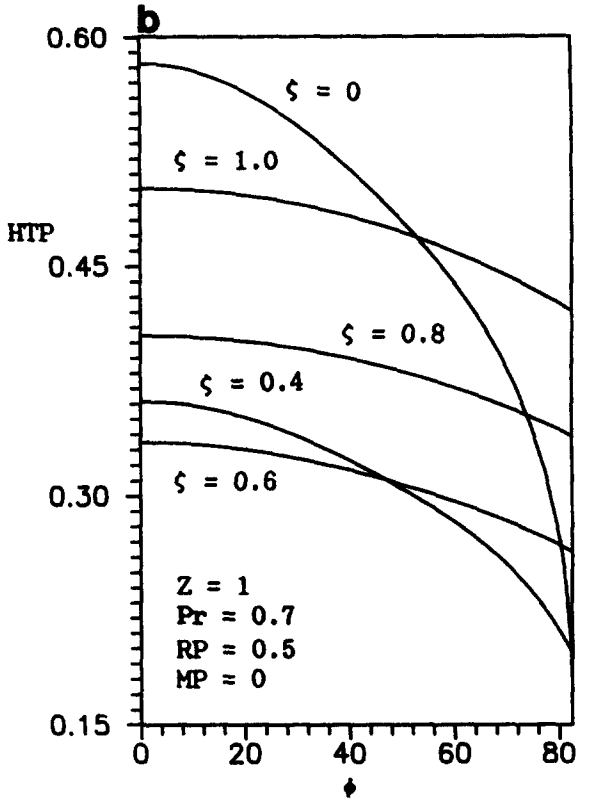

Figure 5b Angular distributions of the heat transfer parameter for a sphere covering the entire free forced-convection range

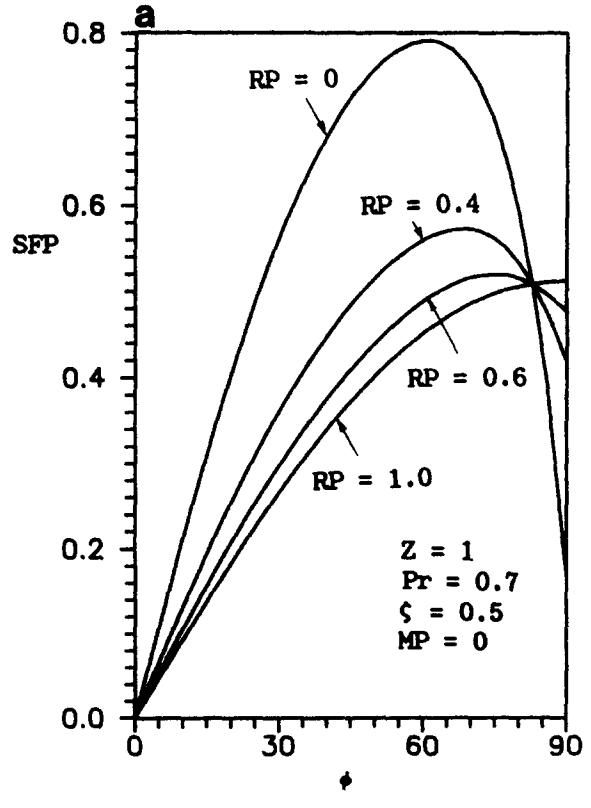

Figure 6a Angular distributions of the skin-friction parameter for a sphere covering the entire forced-convention range from the pure flow forced-convection limit to the pure rotational forced-convection limit

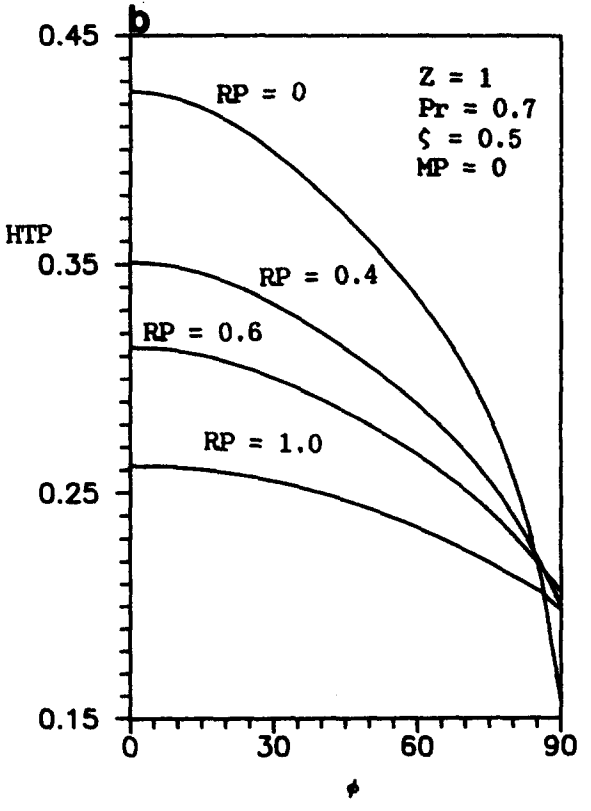

Figure 6b Angular distributions of the heat transfer parameter for a sphere covering the entire forced-convection range from the pure flow forced-convection limit to the pure rotational forced-convection limit

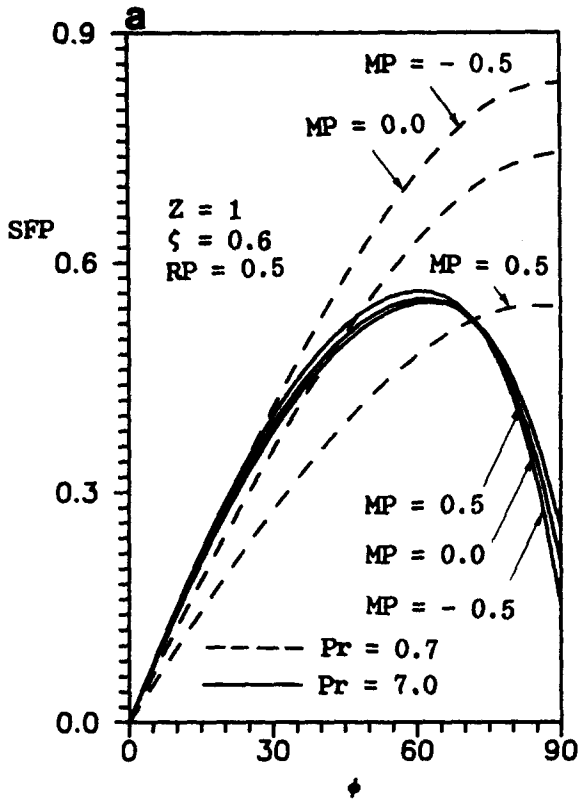

Figure 7a Effects of mass transfer parameter and Prandtl number on the skin-friction parameter

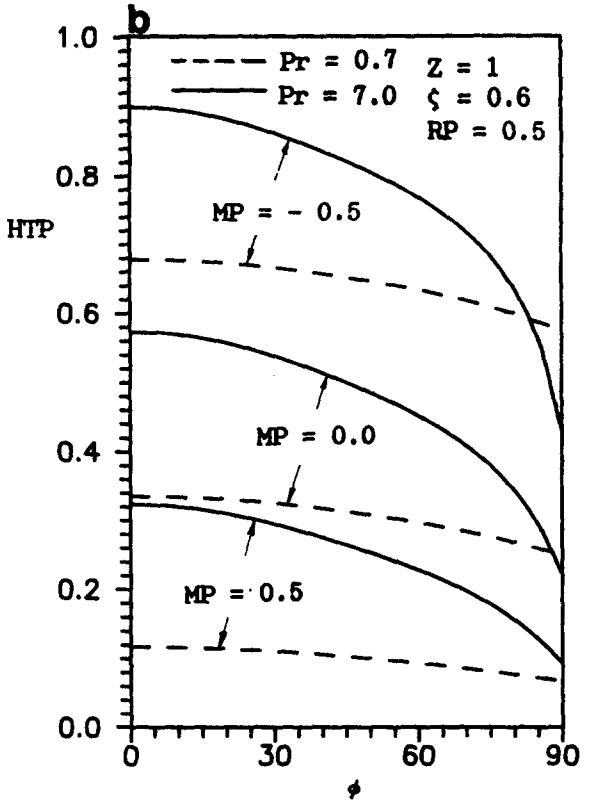

Figure 7b Effects of mass transfer parameter and Prandtl number on the heat transfer parameter

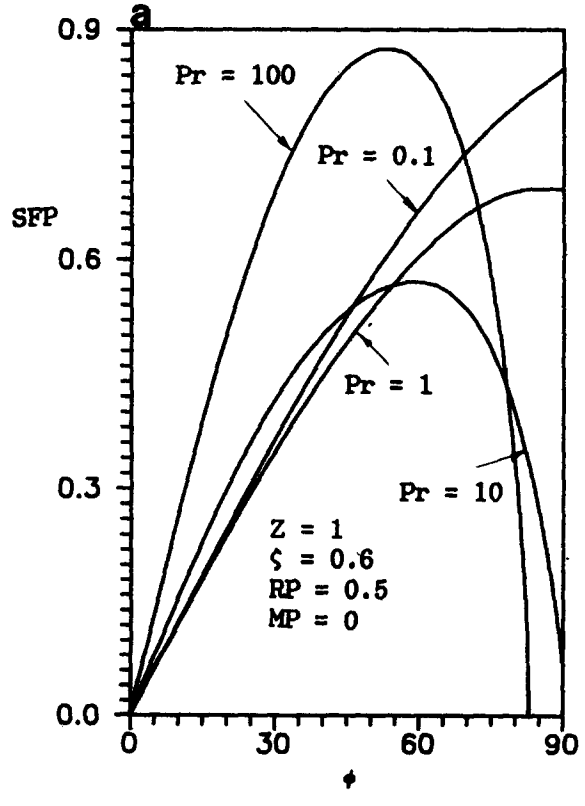

Figure 8a Effect of Prandtl number on the skin-friction parameter

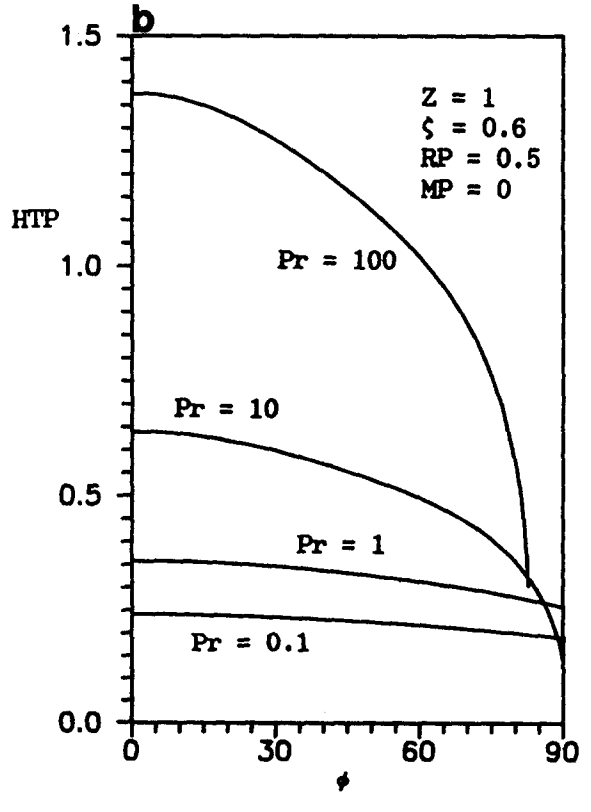

Figure 8b Effect of Prandtl number on the heat transfer parameter

and fluids with smaller thermal diffusivities generate higher dimensionless temperature gradients at the wall.

Conclusions

The nonsimilar boundary-layer analysis of steady laminar mixed-convection heat transfer from an axisymmetric body is extended and unified. The implicit finite-difference solution of the transformed equations is valid for the entire domain of mixed convection from the pure forced-convection limit to the pure free-convection limit and from the pure flow forced-convection limit to the pure rotational forced-convection limit. The validated computer simulation model is successfully applied to the case of mixed thermal convection of a wide range of Prandtl number fluids past a sphere with optional body rotation, fluid suction or injection, and surface heating or cooling mode.

Acknowledgments

The author would like to express his sincere appreciation to the reviewers for their constructive and valuable suggestions.

References

Cebeci, T. and Bradshaw, P. 1977. *Momentum Transfer in Boundary Layers*. Hemisphere, Washington, DC

Chao, B. T. and Greif, R. 1974. Laminar forced convection over rotating bodies. *ASME J. Heat Transfer*, **96**, 463–466

Huang, M. J. and Chen, C. K. 1987. Laminar free convection from a sphere with blowing and suction. *ASME J. Heat Transfer*, **109**, 529–532

Kleinstreuer, C. and Wang, T. Y. 1989. Mixed convection heat and surface mass transfer between power-law fluids and rotating permeable bodies. *Chem. Eng. Sci.*, **44**, 2987–2994

Lee, M. H., Jeng, D. R., and De Witt, K. J. 1978. Laminar boundary layer transfer over rotating bodies in forced flow. *ASME J. Heat Transfer*, **100**, 496–502

Lien, F. S., Chen, C. K., and Cleaver, J. W. 1986a. Forced convection over rotating bodies with blowing and suction. *AIAA J.*, **24**, 854–856

Lien, F. S., Chen, C. K., and Cleaver, J. W. 1986b. Mixed and free convection over a rotating sphere with blowing and suction. *ASME J. Heat Transfer*, **108**, 398–404

Rajasekaran, R. and Palekar, M. G. 1985. Mixed convection about a rotating sphere. *Int. J. Heat Mass Transfer*, **28**, 959–968

Wang, T. Y. 1991. General analysis of thermal convection heat transfer on a vertical cone. *J. CSME*, **12**, 227–232

White, F. M. 1974. *Viscous Fluid Flow*. McGraw-Hill, New York, 345–346